11-15-2006

Effect of Counterface Roughness on the Cross-Path Wear of Ultra-High Molecular Weight Polyethylene

Mary Turell

EFFECT OF COUNTERFACE ROUGHNESS ON THE CROSS-PATH WEAR OF ULTRA-HIGH MOLECULAR WEIGHT POLYETHYLENE

A Thesis Submitted to the
Yale University School of Medicine
in Partial Fulfillment of the Requirements for the
Degree of Doctor of Medicine

by

Mary Elizabeth Turell

2006

EFFECT OF COUNTERFACE ROUGHNESS ON THE CROSS-PATH WEAR OF ULTRA-HIGH MOLECULAR WEIGHT POLYETHYLENE

Mary E. Turell, Anuj Bellare, Thomas S. Thornhill. Department of Orthopedic Surgery, Brigham and Women's Hospital, Boston, MA. (Sponsored by Gary E. Friedlaender, Department of Orthopaedics and Rehabilitation, Yale University School of Medicine).

Ultra-high molecular weight polyethylene (UHMWPE) is used worldwide as a bearing material in total joint replacement prostheses. Despite its excellent biocompatibility and high wear resistance, wear of UHMWPE components continues to be a major problem limiting the clinical lifespan of UHMWPE-containing orthopaedic implant devices. Multi-directional motion or cross-path motion is known to affect wear rates of UHMWPE in total knee and hip replacement prostheses. The purpose of this study was to quantify the effect of counterface roughness on the cross-path wear of UHMWPE and to determine if the previously established unified theory of wear model could accurately predict wear rates in an abrasive wear environment. UHMWPE pins were articulated against both smooth (centerline roughness, Ra, of 0.015 μm) and rough (Ra = 0.450μm) cobalt-chromium counterfaces in a series of six rectangular wear paths (width = *A*, length = *B*) with systematically increasing aspect ratios (*B*/*A*) and linear tracking (*A* = 0), all with identical path lengths (20mm) per cycle. Gravimetric weight loss was converted into volumetric wear rates and wear factors, *k*. The results showed that for both smooth and rough-counterface tests, wear reached a maximum when a 3mmx7mm wear path was employed. The unified theory of wear was generally accurate in predicting wear rates; however, for rough-counterface tests there was a larger increase in the wear factor for higher aspect ratio rectangular wear paths. The ratio [*k* rough/ *k* smooth] decreased monotonically as a function of increasing width of rectangles, normalized by total path length, or $A/(A+B)$. This study showed that wear of UHMWPE articulating in a rectangular motion path likely occurs via a two-step mechanism beginning with molecular orientation followed by material fracture from the UHMWPE surface. The model's inability to accurately predict UHMWPE wear for rectangular paths with lower aspect ratios suggests that there may be other operative wear mechanisms including significant re-orientation in the perpendicular sliding direction. In conclusion, it is possible to predict the wear behavior of UHMWPE using mathematical models. A robust model would have an important role in characterizing and predicting performance of currently used and potential future orthopaedic implant materials.

ACKNOWLEDGEMENTS

I would like to thank my thesis advisors Anuj Bellare and Thomas Thornhill from Brigham and Women's Hospital, Harvard Medical School, and Gary Friedlaender from Yale University School of Medicine. I am grateful to each of these individuals for supporting me in this research, for contributing their perspectives and sharing their expertise, and for broadening my own understanding of research in the area of orthopaedic implant materials. Most importantly, I would like to thank these individuals for being tremendous role models and mentors before and during my years at Yale. I am very appreciative to Dr. Jonathan Grauer and the Orthopaedics and Rehabilitation Department Thesis Committee at Yale University School of Medicine for their critique and review of my thesis. I would like to thank Dr. Valentine Njike, from the Yale-Griffin Prevention Research Center, for contributing his expertise and assistance with statistical analysis. I would also like to acknowledge Dr. Aiguo Wang, at Stryker Howmedica Osteonics, for providing materials including the cobalt-chromium disks that were used as articulation counterfaces in this study. This project was funded through several grant sources including a biomedical engineering grant provided by the Whitaker Foundation, a medical student research grant provided by the Orthopaedic Research and Education Foundation, and a summer research fellowship provided by the Yale University School of Medicine Office of Student Research.

TABLE OF CONTENTS

Figures and Tables

INTRODUCTION

Advances in artificial joint technology have resulted in successful surgical treatments for the debilitating loss of mobility caused by joint disease, traumatic injury, and overuse of native joints. British orthopaedic surgeon Sir John Charnley, M.D., is credited with pioneering some of the earliest artificial joint implant designs that have evolved into the current devices used in contemporary total joint arthroplasty. In 1958, at the Center for Hip Surgery at Wrightington, England, Charnley introduced his low-friction hip replacement. In the first Charnley models, poly(tetrafluoroethylene), or PTFE, was chosen to serve as the polymeric bearing or articulation surface. The design consisted of a PTFE acetabular element that articulated against a PTFE femoral component [1]. Although these artificial joints initially appeared to be very promising in their ability to restore mobility to patients with joint disease, wear damage of PTFE components ultimately proved to limit their clinical utility. The formation of PTFE wear debris within the joint space elicited a strong immunologic inflammatory response and subsequently the need to surgically revise nearly all of the implanted joints less than three years after their original implantation [1]. In 1962, Charnley discontinued the use of PTFE as a bearing surface, and instead employed ultra-high molecular weight polyethylene (UHMWPE) with the hopes of increasing the clinical lifespan of his artificial joint prostheses [1].

Charnley's surgical implantation of artificial joints began to receive international recognition, and orthopaedic surgeons from around the world traveled to Wrightington, England, to learn his techniques. During the 1980's, the number of total hip replacement

(THR) procedures experienced rapid growth and, in recent years, this procedure has continued to gain popularity. Today, while multiple artificial hip joint implant designs exist, the most widely accepted configuration consists of a metallic femoral component that articulates against an acetabular cup with a polymeric bearing surface. Ultra-high molecular weight polyethylene is used worldwide as a polymeric bearing surface in total joint replacement prostheses. Currently, there are approximately 570,000 primary THR and total knee replacement (TKR) surgeries performed in the United States on an annual basis [2]. The American Academy of Orthopedic Surgeons has predicted that the number of THR and TKR procedures performed in the United States is expected to increase to at least 750,000 procedures performed annually by the year 2030 [3].

Multiple aspects of UHMWPE make this polymer ideally suited to serve as a bearing surface in artificial joint replacement prostheses. Combined with the property of excellent biocompatibility, the unique morphology of UHMWPE makes it exceptional in comparison to other polymers and contributes to its ability to withstand the rigorous loading conditions encountered by joint components in the course of daily activity. Each molecule of UHMWPE contains more than 200,000 ethylene units, yielding an overall molecular weight of 3–6 million g/mol [3]. The carbon backbone of UHMWPE can fold in an orderly fashion to form crystalline lamellae (sheet-like structures) embedded within amorphous (disordered) chain regions. Commercially available, processed UHMWPE is generally comprised of approximately 50% crystalline regions and 50% amorphous chain regions. The size and orientation of crystalline regions within the polymer depends on multiple factors including molecular weight and processing conditions. The dense entanglement network associated with the polymer's high molecular weight imparts

superior fracture toughness [4, 5] and high wear resistance to UHMWPE, making it an attractive choice as a bearing surface in both THR and TKR prostheses.

The clinical performance of artificial joint implants and the pattern of wear and surface damage depend on several factors. These include surgical technique, artificial joint implant design, and selection of joint implant materials. Additionally, a variety of patient variables including age, weight distribution, activity level and gait pattern affect clinical performance. Based on the Swedish hip registry, it has been estimated that greater than 90% of total joint replacements with UHMWPE bearing components survive for more than 10 years [6]. UHMWPE-containing artificial joint implants tend to be revised at a rate of about 1% per year in the first decade after implantation [6]. The rate of implant survival declines after 10 years, particularly for patients who are less than 55 years of age [6].

Despite its superior mechanical toughness and high resistance to wear (excellent tribological properties), wear damage of UHMWPE continues to be the leading factor that limits the clinical lifespan of implanted THR and TKR prostheses. The volumetric wear rate of an acetabular cup articulating against a 32mm femoral head has been estimated to be $80mm^3$/year, which translates into an average linear wear rate of 0.1mm annually [7–10]. The thickness of UHMWPE components is typically 1cm or more. Therefore, it would theoretically take 100 years or more for the UHMWPE surface of an acetabular cup to wear through. While this estimate eliminates the likelihood that UHMWPE implant components are in any significant danger of wearing through over the course of an individual's lifetime, other related effects of wear processes are a realistic concern for severely limiting the clinical lifespan of artificial joints. For example, for the

observed clinical wear rates of UHMWPE joint components, billions of sub-micron wear debris particles are produced annually [11,12], which continues to be a primary concern in THR prostheses. The accumulation of particulate wear debris in the joint space and peri-prosthetic tissue can elicit a biological response leading to bone loss (osteolysis) and implant loosening, necessitating complicated revision surgery to replace the implant [13–15]. Osteolysis associated with particulate wear debris has prompted numerous investigations, which study the size, shape, and morphology of particulate debris and the biological pathway that leads to particle-induced osteolysis. Wear debris collected from peri-prosthetic tissue in joint retrieval studies has shown that the majority of debris particles associated with THR prostheses are micron or sub-micron in size and that the particle morphology can generally be categorized as either fibrillar or particulate in shape [16–20]. Particulate wear also occurs in TKR components, although the particle size distribution of wear debris differs from that observed in THR prostheses. TKR particles have been shown to be generally larger than THR wear particles [21]. The effect of wear debris particle size and morphology is an area that is actively being investigated. It has been shown that even given an overall smaller volume of wear debris particles, that smaller sized particles generally have the potential to elicit a stronger biologic inflammatory response than do an equal or larger volume of debris particles of a larger size distribution [22].

In the past, computational and experimental studies aimed at describing the wear behavior of UHMWPE have shown that multi-directional motion or “cross-shear” motion affects the wear rate of UHMWPE in THR and TKR devices [23, 24]. Linear tracking motion, whether unidirectional or reciprocating, produces an extremely low wear rate,

and in fact produces two to three orders of magnitude less wear than is observed clinically in TKR prostheses [24–29]. The higher clinical wear rates observed in TKR and THR prostheses can be attributed to both counterface scratching [30, 31] and the effects of cross-shear motion. In an artificial joint implant, the wear environment is created by implant components that must articulate against one another, and wear occurs at the contact point between components. Wang and colleagues have proposed that in a wear-inducing environment, at the contact point of articulating components, the UHMWPE surface molecules orient preferentially along the principal direction of sliding [24, 27–29]. Unlike in linear tracking, where orientation results in strain hardening of surface material and ultimately increases wear resistance as sliding progresses, in multi-directional motion, the wear surface experiences both compressive and shear forces in multiple directions. As sliding proceeds, the UHMWPE wear surface may strengthen along the direction of sliding, while it weakens in the transverse direction.

It has been demonstrated that the trajectory of motion at the contact point between a femoral head of an orthopaedic implant and an acetabular cup is a quasi-ellipse or an approximate rectangle during a gait cycle [23, 24, 32]. This trajectory of motion differs among individuals. Some individuals have either more elongated (or approximately rectangular) trajectories, while others have more closed (or approximately square) motion patterns [32]. Examples of elongated and closed-motion patterns traced by the contact point between femoral and acetabular components are illustrated in Fig.1. Bennett et al. have postulated that variances in gait patterns, and therefore the differences in motion patterns, affect the *in vivo* wear rates of UHMWPE acetabular cups in patients where other factors such as age, weight, and body proportion are similar [32].

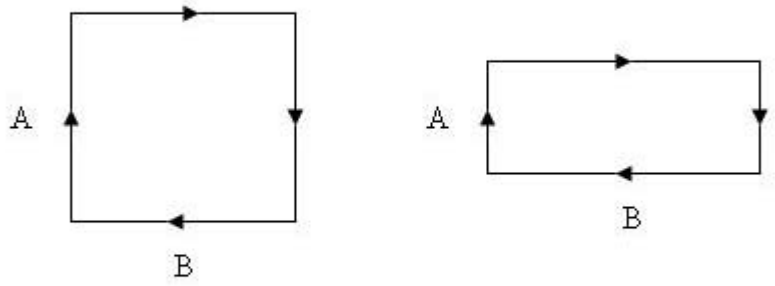

Figure 1: Closed motion pattern (left) and elongated motion pattern (right) with sides *A* and *B* traced by the contact point between the femoral and acetabular components of orthopaedic implants. Arrows represent clockwise direction of sliding motion.

The multi-directional sliding, or orientation-softening wear model, proposed by Wang has been termed the unified theory of wear for UHMWPE [33]. The unified theory of wear proposes that when a femoral head slides against an acetabular cup along the wear path defined by a rectangular loop (with sides of length *A* and *B*), frictional energy is dissipated in both the *A* and *B* directions (see Fig. 1). Since *A* represents the shorter of the two sides of the rectangular loop, *B* defines the principal direction of sliding motion while *A* is secondary. Previous studies have indicated that motion in the principal sliding direction, *B*, leads to plastic deformation or macromolecular orientation, whereas motion in the secondary direction, *A*, leads to material removal by shear [24, 27–29, 33].

Therefore, only energy released in the *A* direction is directly responsible for wear [33]. Based on these observations, the wear rate of UHMWPE can theoretically be quantified and expressed by the following equation:

$$V \propto \mu P(2A) \qquad \text{(Equation 1)}$$

where, *V* represents the volumetric wear rate, μ is the coefficient of friction, *P* is the applied normal load and *2A* is the total sliding distance in the secondary direction per cycle. In order to compare wear rates over time for various materials, wear is often expressed as a wear coefficient or wear factor, *k*.

The wear factor, *k*, is defined as:

$$k = \frac{V}{P * d} \qquad \text{(Equation 2)}$$

where, *V* represents the volumetric wear rate, *P* is the applied normal load, and *d* represents total sliding distance. In the case of a rectangular wear path with dimensions *A* and *B*, the wear factor, *k*, can be written as:

$$k = \frac{V}{P(2A+2B)} \propto \frac{\mu P(2A)}{P(2A+2B)} \propto \frac{A}{A+B} \qquad \text{(Equation 3)}$$

By using equation 3, it is theoretically possible to quantify the effect of cross-path motion on the wear rate, and the wear factor of UHMWPE.

In a previous set of experiments, wear factors were compared for UHMWPE pins articulated against cobalt-chromium disks polished to implant grade smoothness (centerline roughness, Ra, of 0.015μm) [34]. In this study, a series of rectangular wear paths were compared such that the side lengths *A* and *B* of the rectangular loop were systematically increased but the total path length remained constant at 20mm. In other words, in this series of graded rectangular wear paths, only the aspect ratio of the wear path was systematically changed, but the overall distance of the rectangular loop remained constant. This series of wear path geometries is diagrammatically illustrated in Fig. 2. The results showed that the wear factors from these experiments were in general

Wear Path	Motion Pattern	Aspect Ratio	A/A+B
5mmx5mm		1.00	0.5
4mmx6mm	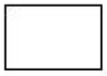	1.50	0.4
3mmx7mm	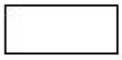	2.33	0.3
2mmx8mm	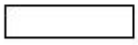	4.00	0.2
1mmx9mm	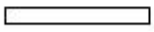	9.00	0.1
0mmx10mm		∞	0.0

Figure 2: Rectangular wear path geometries and associated aspect ratios and ratio of A/A+B. Note that the total path length is 20mm for all wear path geometries.

agreement with the proposed unified theory of wear model proposed by Wang and colleagues only at high aspect ratios [34]. As anticipated, wear factors were found to significantly decrease when the rectangular wear path had the highest aspect ratio (or more elongated rectangular wear path) and in the case of linear tracking [34].

A question that remains to be answered is whether the unified theory of wear remains valid under conditions of abrasive wear. Previous studies have shown that the addition of bone cement particles (with zirconium and barium sulfate particulate additives required to make bone cement radio-opaque) and the presence of bone particles within the wear test serum lubricant produce significantly greater surface damage to stainless steel articulation counterfaces, which in turn results in surface roughening and increased wear rates [30]. Similarly, other authors have found that roughening of the femoral head, to a degree seen clinically in retrieval specimens, can increase the observed variability of volumetric wear rates approximately seven-fold. This fact may explain why random femoral head scratching *in vivo* accounts for otherwise difficult to explain variations in wear rates as abrasive wear may be a key factor causing excessive wear in the most problematic subset of the patients with total joint replacements [31]. The purpose of the current study is to determine whether the unified theory of wear remains valid under conditions of abrasive wear. The abrasive wear environment in this study was created by UHMWPE pins articulating against a roughened cobalt-chromium counterface and using rectangular wear paths of varying aspect ratios.

HYPOTHESIS

The purpose of this study was to determine whether the unified theory of wear, proposed by Wang and colleagues, could accurately describe the wear behavior of UHMWPE in an abrasive wear environment. In a previous set of experiments, the unified theory of wear generally described the wear behavior of UHMWPE in an environment in which UHMWPE pins were articulated against cobalt-chromium disks polished to implant grade smoothness. Determining if the current model would predict the wear behavior of UHMWPE under abrasive conditions is important as an abrasive wear environment more closely mimics the environment which UHMWPE implant components are exposed *in vivo*. It was hypothesized that wear of UHMWPE would be dependent upon both wear path geometry as well as counterface roughness. In addition, it was hypothesized that under conditions of abrasive wear, the unified theory of wear model would describe the cross-path wear behavior of UHMWPE as accurately as it had in the previous study that employed smooth counterfaces.

MATERIALS AND METHODS

UHMWPE starting material

Commercially available, ram-extruded GUR 1050-medical grade (Hoechst-Ticona, Bayport, TX) UHMWPE rod stock (PolyHi Solidur, Ft. Wayne, IN) was used as the starting material for all wear tests. The original rod stock had a diameter of 7.6 cm and was subsequently machined into cylindrical wear testing pins with overall dimensions of 20mm in length and 9mm in diameter for all tests. All UHMWPE pins were subjected to wear tests in the as-machined condition. In other words, no additional cross-linking or pre-sterilization processing steps were added following the receipt of the original starting polymer.

Wear testing protocol and apparatus

All wear tests were conducted using a six-station pin-on-disc OrthoPOD^{TM} (Advanced Mechanical Technology, Inc., Watertown, MA) multi-directional wear tester. This particular model of wear testing apparatus was designed specifically to study and compare wear behavior of orthopaedic implant materials. A successful history of wear testing using this device had been previously established at multiple academic centers nationally and internationally [35-37]. A series of six different articulation or wear path patterns were manually digitized into the OrthoPOD^{TM} multi-directional wear tester. These six articulation patterns included: a square with dimensions of 5mm×5mm, four rectangles with dimensions of 4mm×6mm, 3mm×7mm, 2mm×8mm, and 1mm×9mm, and a linear tracking pattern with dimensions of 0mm×10mm. In each case, the total

tracking distance was 20mm (i.e., the total distance of the rectangular perimeter) for each of the digitized articulation patterns (Fig. 2). While total path length remained constant at 20mm, the difference between the six articulation patterns was in the various aspect ratios of the square or rectangular path. For each wear test, the OrthoPOD^{TM} multi-directional wear tester was loaded with six UHMWPE pins as shown in the experimental set-up in Fig. 3. All wear tests were conducted at a cycle frequency of 1Hz (constant sliding speed of 20mm/sec along the wear track). A constant applied load of 192N or an applied stress of 3MPa was used. This load was chosen as it is well within the physiological range of 2–5MPa seen clinically for the hip joint [38, 39]. All wear tests were conducted for a duration of at least one million cycles.

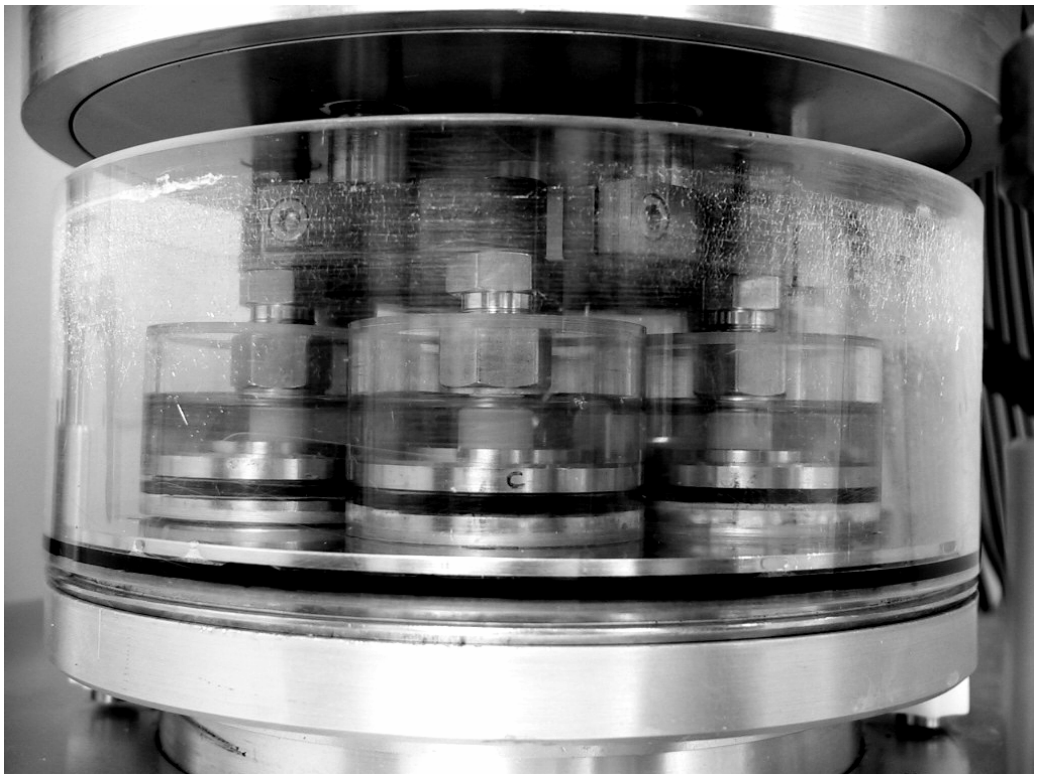

Figure 3: Experimental set-up showing OrthoPOD^{TM} (Advanced Mechanical Technology, Inc., Watertown, MA) 6-station multi-directional wear tester.

Wear test serum lubricant: A bovine serum lubricant was used for all wear tests. Properties and overall composition of test serum lubricant, in particular serum protein concentration, are known to affect *in vitro* wear rates in simulator testing [40-42]. Studies performed by Wang and colleagues demonstrated that serum protein concentrations of 20-30g/dl are required to produce physiologic levels of wear in simulator testing [43]. The composition of the serum lubricant used in this study followed the previously established and validated formulations proposed by Wang and colleagues [43]. Specifically, bovine calf serum with a protein concentration of 7.9g/dL (JRH Biosciences) was diluted as follows. For 100ml of lubricant, 29.1ml of JRH calf serum was mixed with 60.9ml of distilled water and 10.0ml of 200mM stock EDTA solution. Additionally, 0.2g of sodium azide was mixed into the solution for its bactericidal effects. This protocol yielded final serum lubricant parameters of 23g/L protein, 20mM EDTA, and 0.2% sodium azide. The bovine serum lubricant temperature was strictly maintained at 37°C using a re-circulating heated water bath.

Wear test cobalt-chromium disks: Cobalt–chromium disks with dimensions of 25mm diameter and 3mm thickness were used as the articulation counterface. Two series of wear tests using each of the six experimental articulation patterns were performed. In one series of tests, cobalt–chromium disks were polished to implant-grade surface finish with a centerline roughness of 0.015μm (Ra). Surface roughness was measured using a Taylor Hobson Surtronic 3+ diamond stylus profilometer (Taylor Hobson, Leicester, UK). At least 10 measurements were made from each disk in different directions and locations. In a second set of experiments, the cobalt–chromium disks were scratched along random directions using 320 grit emery paper in accordance with the previously established

method of Wang et al., resulting in an average centerline roughness, Ra, of 0.450μm [44]. Briefly, this method entails manually scratching the disks in random directions using emery paper wetted with distilled water. Disks were inspected carefully to be sure that scratches were randomized and that no orientation of scratch patterns existed. Disks were thoroughly rinsed in distilled water to remove metallic debris and dried in a vacuum oven prior to use. A total of six UHMWPE pins plus an additional pin serving as a soak control were used for all wear tests.

Data collection and analysis

The UHMWPE wear rate for each of the six wear path geometries was determined in for both the set of experiments in which smooth (implant grade) cobalt-chromium counterfaces were employed and for the second series in which rough counterfaces were used. Wear rate was determined by measuring the gravimetric weight loss (in milligrams) per pin at approximately every 200,000 cycles. Prior to being weighed, UHMWPE pins were first washed to remove residue from the bovine serum lubricant. Pins were washed twice with distilled water followed by an alcohol and acetone rinse, respectively. The pins were subsequently dried in air at 25°C for 15 min prior to determination of weight loss. It should also be noted that the soak control pin consistently revealed that the amount of absorption of bovine serum by the UHMWPE pin specimen was undetectable and therefore any corrections to compensate for fluid absorption were unnecessary. Gravimetric weight loss was further converted into volumetric wear data by using the density value of 0.943 g/cm^3 for UHMWPE [45]. Wear factor values, k, were then calculated for each pin as follows:

$$k = \frac{V}{P(2A + 2B)} \qquad \text{(Equation 4)}$$

where, k represents the wear factor, V is the calculated volumetric wear in mm^3, P is the applied normal load (192 Newtons), and $2A+2B$ is the total sliding distance in meters (i.e., 20mm times the total number of cycles completed). A mean wear factor value was determined for each of the six wear path geometries for both the series of rough and the series of smooth-counterface tests by taking the average of all wear factor values calculated in each group.

Statistical Analysis

All data were entered in excel spreadsheet and analyzed using SAS software for Windows version 9.1 (SAS Institute, Cary, NC). Wear factor data were first analyzed using a univariate procedure to verify that the data met criteria for normal distribution. The data met criteria for normal distribution; parametric statistics were applied to analyze these data. One-way ANOVA were used to assess differences in the means of wear factors between rough versus smooth counterfaces for each wear path geometry tested. One-way ANOVA including Duncan's Multiple Range Test were also used to evaluate differences in the means of wear factors for the six wear path geometries for each counterface (smooth and rough) test series. Two-way ANOVA was employed to assess interaction between counterface roughness and wear path geometry. Linear regression was used to evaluate the linear trend of the mean wear factors as the wear path geometry

changed for the smooth and rough-counterface series. Statistical significance was determined by a two-tailed p-value < 0.05.

RESULTS

Effect of Wear Path Geometry

Wear tests showed that the wear factor, *k*, increased incrementally as a function of wear path geometry within the aspect ratio range from infinity to 2.3 (0mm×10mm to 3mm×7mm wear path). Interestingly, for both smooth and rough-counterface tests, the volumetric wear rate reached a maximum when a 3mm×7mm wear path (aspect ratio= 2.3) was used (Fig. 4). For the smooth-counterface test series, the maximum wear factor was 2.45E-06 ± 6.26E-07 (mean ± S.D.). For the rough-counterface test series, the maximum wear factor was 3.87E-06 ± 1.57E-06 (mean ± S.D.).

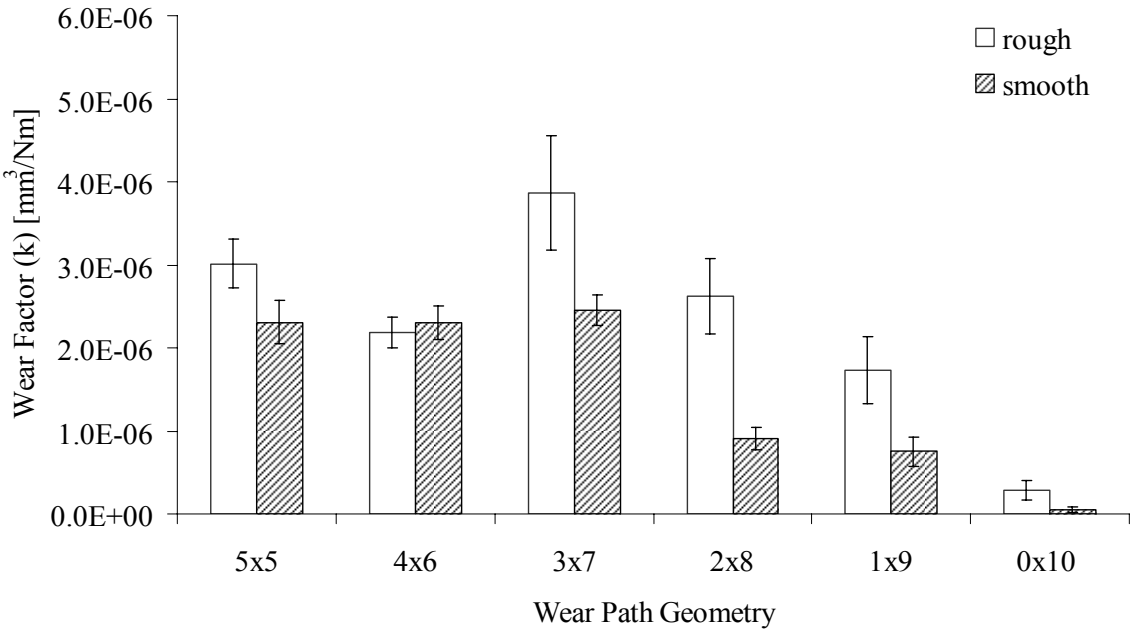

Figure 4: Comparison of wear factors, *k*, for both rough and smooth cobalt-chromium counterfaces for six different wear path geometries (mean ± 95% confidence interval)

The Linear regression model revealed a linear trend in the mean wear factors for the smooth and rough-counterface series (intercept p-value=0.0045 and 0.0042 for the smooth and rough-counterface series respectively). The strength of association was greatest with the smooth-counterface series (R^2=0.64). This trend existed despite the observed maximum wear reached when the 3mm×7mm wear path geometry was used. In the rough-counterface series, the strength of association was not as strong (R^2=0.31) as it was for the smooth-counterface series.

The differences between mean wear factors, *k*, as a function of wear path geometry (0mm×10mm to 5mm×5mm) were analyzed within the series of smooth-counterface tests. This analysis was then repeated for within the rough-counterface series. A summary of the mean wear factors, *k*, showing which means are significantly different from one another within the smooth-counterface series are shown in Table 1. The same summary for the rough-counterface series is also shown in Table 1.

Table 1: Effect of wear path geometry on the wear factor, *k*, for tests conducted with smooth and rough-counterfaces*

Wear Path Geometry	***k* Smooth** mean ± S.D.	(*)	***k* Rough** mean ± S.D.	(*)
0mm×10mm	5.06E-06 ± 1.12E-07	(c)	2.87E-07 ± 2.76E-07	(E)
1mm×9mm	7.50E-07 ± 4.32E-07	(b)	1.74E-06 ± 9.13E-07	(D)
2mm×8mm	9.09E-07 ± 3.92E-07	(b)	2.62E-06 ± 1.03E-06	(B,C)
3mm×7mm	2.45E-06 ± 6.26E-07	(a)	3.87E-06 ± 1.57E-06	(A)
4mm×6mm	2.31E-06 ± 5.53E-07	(a)	2.19E-06 ± 5.20E-07	(C,D)
5mm×5mm	2.30E-06 ± 6.50E-07	(a)	3.01E-06 ± 9.47E-07	(B)

*For both smooth and rough-counterfaces, wear path geometries denoting the same letter were not significantly different from each other (p>0.05 using single-factor ANOVA-DMRT).

Smooth-counterface Series:

Within the smooth-counterface test series, the wear factor, *k*, was dependent upon the wear path geometry used. Single-factor ANOVA-DMRT demonstrated that differences in the mean wear factor, *k*, at different wear path geometries were statistically significant ($p<0.05$). Within the smooth-counterface test series, the experimentally observed wear factor, *k*, for the 5mm×5mm square path was 2.5 times greater than the wear factor resulting when a 2mm×8mm path was used ($p< 0.05$, ANOVA-DMRT), which agrees well with the prediction given by the unified theory of wear and mathematically expressed by equation (3). In other words, the A/(A+B) ratio for the 2mm×8mm wear path is 0.2 and for the 5mm×5mm wear path this ratio is 0.5. Therefore the predicted ratio of these two wear factors, *k*, using the unified theory of wear model would theoretically be 2.5 (i.e., 0.5 divided by 0.2 equals 2.5).

Rough-counterface Series:

As with the smooth-counterface experiments, when the wear factor, *k*, was analyzed within the series of rough-counterface tests, *k* was shown to be dependent upon wear path geometry. Single-factor ANOVA-DMRT demonstrated that differences in the wear factor, *k*, at different wear path geometries was statistically significant ($p<0.05$). When comparing the ratio of the wear factors for the 5mm×5mm and the 2mm×8mm wear path geometries within the rough-counterface series, the wear factor for the 5mm×5mm square path was only 1.1 times greater than the wear factor for the 2mm×8mm path. For the rough-counterface test series, the difference between the wear

factors for the 5mm×5mm and the 2mm×8mm wear paths was not significant ($p>0.05$ using single-factor ANOVA-DMRT)(Table 1).

Effect of counterface roughness

When comparing wear factors, *k*, within each wear path geometry, counterface roughness had a substantial effect on wear rate (Table 2). Although standard deviations for the mean wear factors were large, the differences in mean wear factors between rough and smooth-counterface tests were statistically significant in almost all cases ($p< 0.05$ using single-factor ANOVA-DMRT). However, for the 4mm×6mm tests there was no significant difference in wear for the smooth and rough-counterface tests ($p>0.05$ using single-factor ANOVA-DMRT).

Table 2: Comparison of wear factors, *k*, (mean ± S.D.) for rough and smooth cobalt-chromium counterfaces for six different wear path geometries.

Wear Path A×B	***k* Smooth** mean ± S.D. (n)	***k* Rough** mean ± S.D. (n)	**p-value**[A]
0mm×10mm	5.06E-06 ± 1.12E-07 (30)	2.87E-07 ± 2.76E-07 (24)	p<0.05*
1mm×9mm	7.50E-07 ± 4.32E-07 (24)	1.74E-06 ± 9.13E-07 (20)	p<0.05*
2mm×8mm	9.09E-07 ± 3.92E-07 (36)	2.62E-06 ± 1.03E-06 (20)	p<0.05*
3mm×7mm	2.45E-06 ± 6.26E-07 (42)	3.87E-06 ± 1.57E-06 (20)	p<0.05*
4mm×6mm	2.31E-06 ± 5.53E-07 (30)	2.19E-06 ± 5.20E-07 (24)	p>0.05
5mm×5mm	2.30E-06 ± 6.50E-07 (24)	3.01E-06 ± 9.47E-07 (39)	p<0.05*

[A]p-values determined by single-factor ANOVA-DMRT where significance ($p<0.05$) denoted by *

Interaction between counterface roughness and wear path geometry

Two-factor ANOVA-DMRT revealed that there was a significant interaction between wear path geometry and counterface roughness and that this interaction affected the relationship between counterface roughness and the resulting wear factors (Table 3).

Table 3: Two-factor ANOVA-DMRT: Effect of interaction variable (wear path) and counterface roughness on wear factor, *k.*

Sources of Variance	Degrees of Freedom	Sum of Squares	Mean Squares	F-Value	p-value
Counterface[A]	1	5.5E-11	5.5E-11	104.26	p<0.0001
wear path[B]	5	3.1E-10	6.1E-11	116.64	p<0.0001
counterface*wear path	5	2.9E-11	5.8E-12	10.88	p<0.0001
Error	321	1.7E-10	5.3E-13		
Total	332	5.6E-10			

[A]counterface (rough or smooth)
[B]Wear path: defined as 0mm×10mm, 1mm×9mm, 2mm×8mm, 3mm×7mm, 4mm×6mm, or 5mm×5mm

An important finding of this study was that counterface roughness affected wear to a greater extent in experiments in which more linear (higher aspect ratio) rectangular wear path geometries were used as compared to the more square-like wear paths. In comparison to the smooth-counterface series, the rough-counterface tests demonstrated wear rates that were significantly greater than predicted by the unified theory of wear when more linear wear paths were tested ($p<0.05$ using two-factor ANOVA-DMRT). As indicated by an R^2 value= 0.71, there was a decreasing trend in the ratio of wear factors

between rough and smooth-counterface test series (i.e., [*k* rough/*k* smooth]) as the ratio A/(A+B) increased (i.e., as the aspect ratio of the wear path geometry decreased) (Fig. 5).

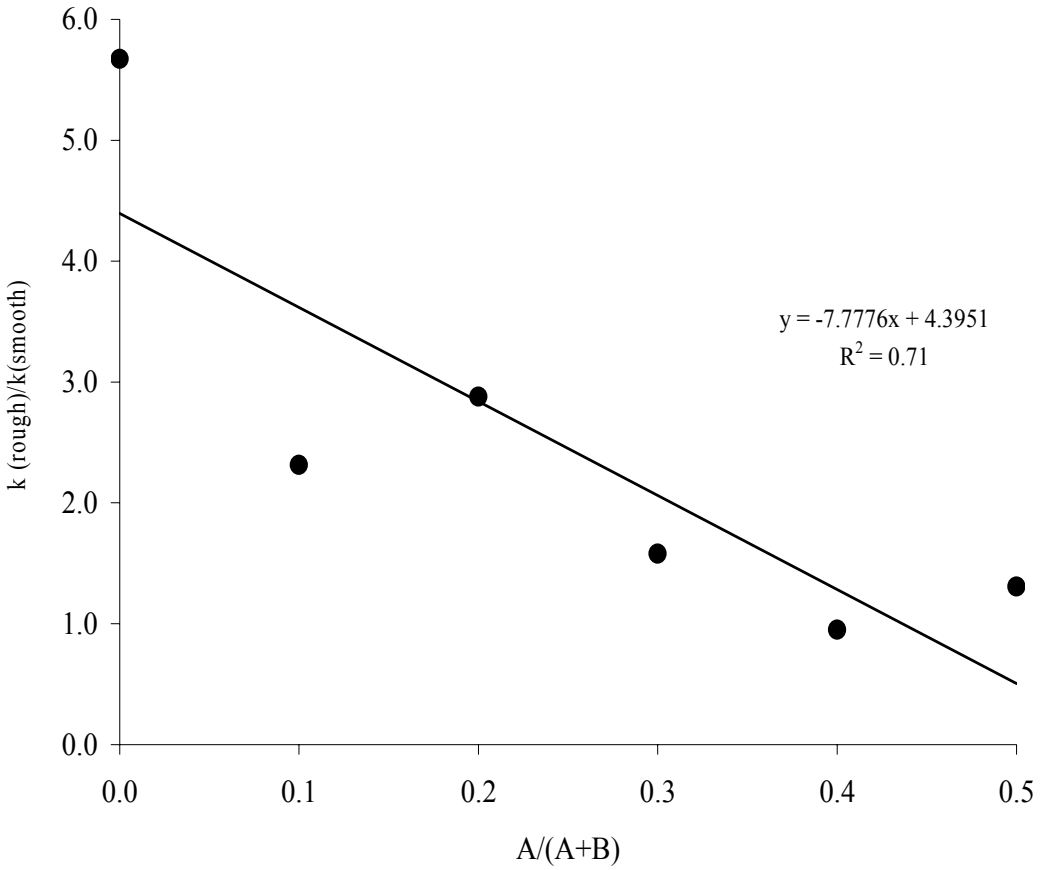

Figure 5: Comparison of wear factor ratios [*k* rough/*k* smooth] as a function of A/A+B. (where "B" represents wear path length, or the principal direction of sliding, and "A" represents wear path width, or the secondary direction of sliding)

Unified theory of wear

In order to assess the validity of the unified theory of wear in predicting the wear rate of UHMWPE based on a particular wear path geometry, the experimentally observed wear factor values for both the smooth and rough-counterface tests were plotted as a function of the ratio $A/(A + B)$. This comparison is shown in Fig. 6. These curves were

then compared to the theoretical wear factor trends predicted using the unified theory of wear, in which the maximum predicted wear factor was taken to be the value of the wear factor obtained from the 5mm×5mm square wear path. Linear regression of the experimentally observed wear factors were included for comparison to the theoretical trends predicted using the unified theory of wear (Fig. 6).

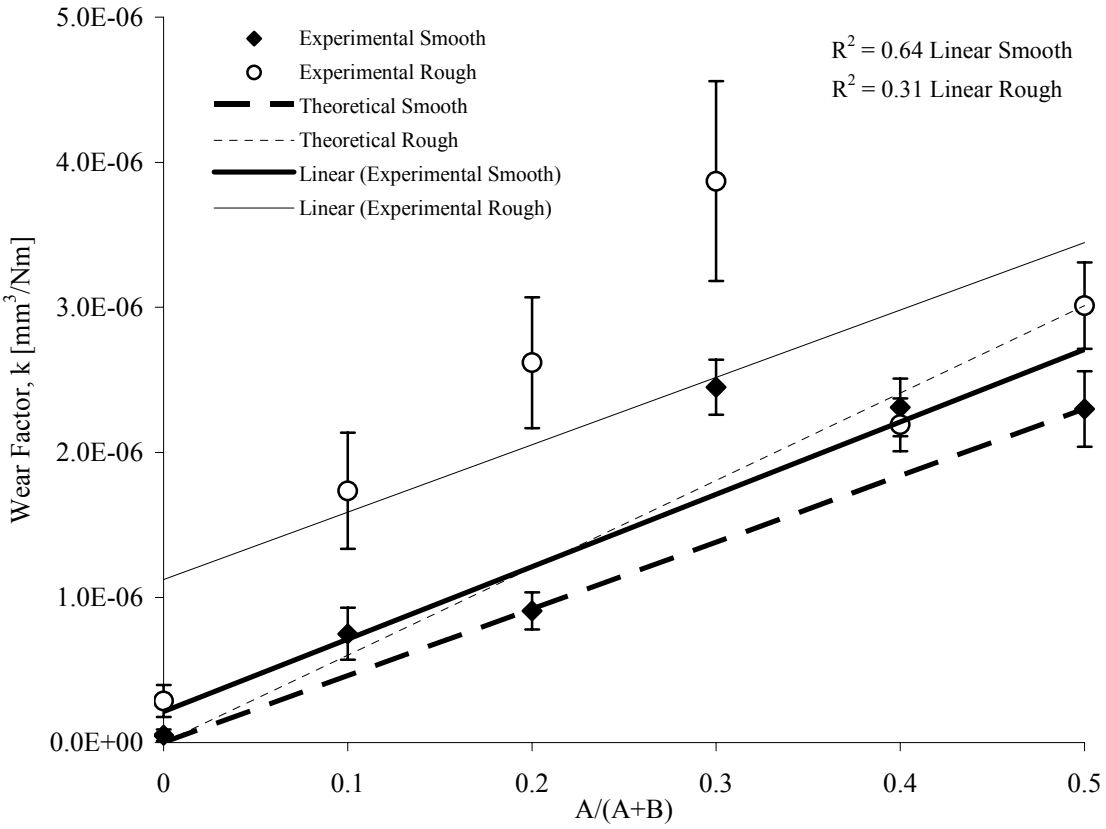

Figure 6: Linear fit for wear factors, *k*, as a function of A/(A+B) ratio (mean ± 95% confidence interval.). Theoretical wear (predicted using unified theory of wear model with maximum *k* assigned at 5mm×5mm path) and linear regression of experimentally observed wear are indicated by solid and dotted lines.

As shown in Fig. 6, the orientation-softening or unified theory of wear was qualitatively better at predicting wear in cases where the aspect ratio of the rectangular wear path was high (i.e. wear paths ranging from 0mm×10mm to 3mm×7mm).The model was unable to accurately predict wear in all cases over the entire range of rectangles for both the smooth and rough-counterface series. In the series of smooth-counterface tests, the unified theory of wear parameter $A/(A + B)$ was particularly accurate in the prediction of wear rates in cases where the aspect ratio of the rectangular path was highest, such as in the 0mm×10mm to 3mm×7mm wear paths. The monotonic increase in wear factors in the $A/(A + B)$ range of 0.0 and 0.3 for UHMWPE in both rough and smooth-counterface tests suggested that a linear correlation between wear factor, k, and $A/(A + B)$ does exist. Therefore, a linear curve fit was conducted in a separate plot (Fig. 7) for the wear factors in the $A/(A + B)$ range of 0.0–0.3. Linear regression analysis in Fig. 7 shows that the wear factor values from both the smooth and rough-counterface tests show a strong linear relationship in this range (R^2=0.88 and 0.99 for smooth and rough-counterfaces, respectively). Therefore, the unified theory of wear model was generally accurate in predicting wear in the $A/(A + B)$ range of 0.0–0.3, or in rectangular wear paths with higher aspect ratios. Linear regression analysis revealed an increase in R^2 from 0.64 to 0.88 in the smooth-counterface series when analyzed over the range of 0mm×10mm to 5mm×5mm and 0mm×10mm to 3mm×7mm, respectively. Similarly, in the rough-counterface series, linear regression revealed an increase in R^2 from 0.31 to 0.99 when analyzed over the range of 0mm×10mm to 5mm×5mm and 0mm×10mm to 3mm×7mm, respectively.

According to the theoretical model of Wang [33], the maximum wear factor should occur at $A = B$ or $A/(A + B) = 0.5$ (5mm×5mm square wear path). Instead, the experimentally observed wear factor peaked at $A/(A + B) = 0.3$ for both smooth and rough-counterface experiments. In fact, the 3mm×7mm showed a 16% increase over the 5mm×5mm square path in the series where rough-counterfaces were employed and this difference was statistically significant ($p < 0.05$, single-factor ANOVA-DMRT).

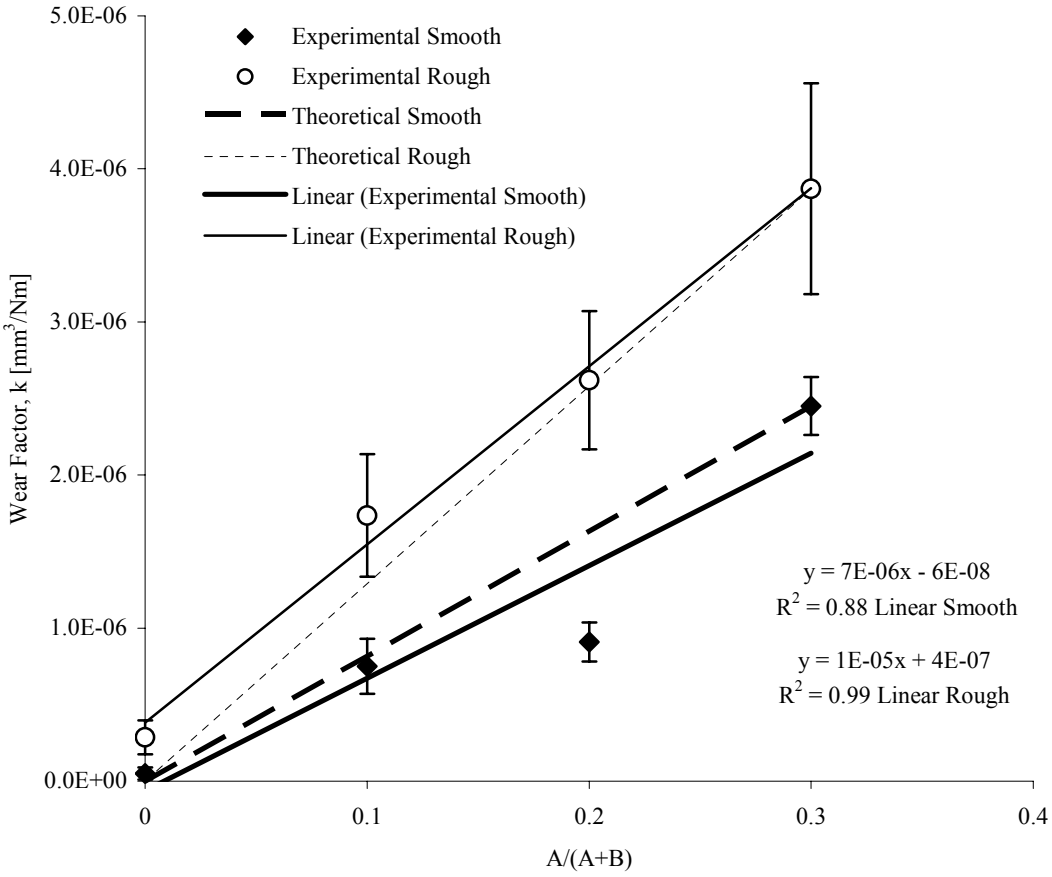

Figure 7: Linear fit (with maximum wear factor, *k*, occurring at A/(A+B) = 0.3) for wear factors as a function of A/(A+B) ratio (mean ± 95% confidence interval). Theoretical wear (predicted using unified theory of wear model with maximum *k* assigned at 3mm×7mm path) and linear regression of experimentally shown wear are indicated by solid and dotted lines.

DISCUSSION

Wear tests

This study was conducted as an extension of a previous study that sought to quantify the effect of the cross-path motion on wear rate of UHMWPE and to compare experimentally observed wear rates with those theoretically predicted by the unified theory of wear model. As the ability of the model to predict wear rates when a series of rectangular wear paths were used with smooth-counterfaces was known, the aim of the present study was to address the effects of counterface roughness on wear rates for different cross-path motions. For a rectangular wear path with a width A and a length B (where $A < B$), the numerical parameter $A/(A + B)$ is a convenient measure to relate wear factor, k, to cross-path motion for rectangles with various aspect ratios, B/A. The numerical parameter $A/(A + B)$, defined by the unified wear model, was generally accurate in predicting that wear rates would increase as a function of decreasing aspect ratio (i.e. as a function of the wear path approaching a square configuration) but only in the range of the 0mm×10mm wear path to the 3mm×7mm configuration. This was trend was demonstrated by linear regression (for aspect ratios ranging from infinity to 2.3 , or 0mm×10mm to 3mm×7mm wear paths) that returned R^2 values of 0.88 and 0.99, for tests with smooth and rough-counterfaces, respectively. In both smooth and rough-counterface groups, wear factors reached a maximum when a 3mm×7mm wear path was employed, and the observed wear factor remained relatively constant as the aspect ratio of the wear path continued to decrease beyond this point (i.e., continued to approach the 5mmx5mm square path).

The failure of the unified wear model to predict wear rates in some cases for both rough and smooth-counterface tests raises questions about some of the underlying assumptions upon which the model is based. For example, for any rectangular wear path with sides *A* and *B*, where $A < B$, the model assumes that orientation on the molecular level occurs in the principal direction of sliding (the *B* direction), while fracture, or the actual wearing of UHMWPE, occurs only in the *A* direction. Based on the results of this study, in which wear reached a maximum for the 3mm×7mm wear path, this assumption may not be a completely valid description of the actual orientation and wear processes. The current model may be an over simplification of the actual wear processes that occurs in rough and smooth wear environments. It is possible that complete orientation and strain hardening of UHMWPE in the principal direction of sliding (*B* direction) is required for wear to occur solely in the *A* direction, and that this is only achieved at 7mm of sliding. It is therefore possible that for the 5mm×5mm and 4mm×6mm wear paths that complete orientation and strain hardening had not yet occurred. Therefore, a significant reorientation may occur in the secondary sliding direction (*A* direction) as well, as opposed to fracture and wear of the fully oriented, strain hardened UHMWPE fibrils. Reorientation of UHMWPE surface molecules would imply that a different wear mechanism is operative since biaxial orientation prior to wear would result in a more sheet-like material wearing from the surface rather than splitting of fibrillar UHMWPE wear debris. Isolation and characterization of the morphology of UHMWPE wear debris particles from this study is an area for future investigation. The aforementioned wear and orientation mechanisms appeared to occur in two discrete ranges of $A/(A + B)$, irrespective of the roughness of the counterface employed. Fig. 7 shows that there was a

linear correlation between wear factor, k, and the numerical parameter $A/(A + B)$, regardless of counterface roughness over the range of aspect ratios from infinity to 2.3 (i.e., linear tracking to a 3mm×7mm wear path geometry). The linear equations for these correlations as well as the R-values (to measure the degree of fit) were obtained for both the smooth and rough-counterface tests. In the equation for a straight line, $k = m[A/(A + B)] + c$, the constant c (y-intercept) represents the fraction of wear factor that is due to linear, abrasive wear and the constant m (slope) is a measure of the dependence of cross-path wear on the wear path geometry. The following equations were obtained for the linear correlations Fig. 7):

$$k = 7\,E-06 * \left(\frac{A}{A+B}\right) - 6\,E-08 \qquad (R^2 = 0.88)$$

(smooth-counterface)

$$k = 1\,E-05 * \left(\frac{A}{A+B}\right) + 4\,E-07 \qquad (R^2 = 0.99)$$

(rough-counterface)

It is evident that the constant c cannot assume a negative value as the component of linear, abrasive wear can not be less than zero. The low, negative wear factor value of 6E−08 for linear tracking using a smooth-counterface obtained from the linear fit is most likely a consequence of experimental error, which can be taken to be zero or replaced by the experimentally measured positive value of 5.06E−08. The value of the slope, m, was greater in the rough-counterface series of wear tests. The ratio of the slopes [m rough/m smooth] was 1.4, revealing that there was a steeper dependence of wear factor, k, on the numerical parameter, $A/(A + B)$, in the case of rough-counterface. For both the smooth

and rough-counterface, the high *R*-values indicated a strong linear correlation between the wear factor and ratio of $A/(A + B)$. The high level of fit of the wear factors in the series of wear paths in the range of 0mm×10mm to 3mm×7mm paths suggests that complete orientation followed by fracture of fibrils was the primary mechanism of wear in both of these cases. This is in close agreement with the mechanism of wear and theoretically predicted pattern of wear outlined by the unified theory of wear model. Independent of the accuracy with which the model investigated in this paper predicted wear rate, the overall experimental results support the hypothesis that wear rate is in fact dependent upon the wear path geometry, counterface roughness and the interplay of these two variables.

Clinical relevance

The finding that UHMWPE wear rate is dependent upon both wear path geometry and counterface roughness has a number of clinically relevant implications. The observation that the differences in wear rates for rough-counterface tests as compared to smooth-counterface tests are accentuated for wear paths with higher aspect ratios (more elongated rectangular patterns) and that these differences systematically decrease as the wear path geometry approaches a square pattern is an important finding. For example, in total joint replacement applications where more linear wear is known to be operative and to have a significant impact upon the lifetime of the joint replacement (i.e., as is the case of the knee joint), the effects of abrasive wear (simulated by a roughened-counterface in this study) are of greater concern. It should be noted that the results of this study reveal a somewhat oversimplification of the wear mechanisms as they occur in clinical

application since the effects of third body wear and fatigue-related wear mechanisms were not investigated.

A question that remains to be answered is whether it may be possible to predict motion path patterns for individuals by conducting gait analysis and if so, whether motion path pattern can be therapeutically manipulated using methods of gait training or by making improvements to implant design. A challenge in addressing these questions lies in the difficulty in assessing gait in patients who require total joint replacement surgery as gait in these individuals may be altered from their normal baseline gait due to the orthopaedic complications, which necessitated surgery in the first place. Similarly, gait patterns in these individuals may be dramatically altered following total joint replacement surgery, making it difficult to predict the effects of implant design in advance of surgery. The extent to which total joint replacement surgery affects the differences in gait pattern observed before and after joint replacement surgery is not known.

Limitations

The results of this study represent an attempt to quantify the effect of cross-path motion path pattern and counterface roughness on the wear rate of UHMWPE. It should be noted that the data, in particular the wear factor values, that have been analyzed in this paper represent the results of preliminary wear tests conducted for each wear path geometry to a period of at least one million cycles. A more comprehensive study, and one that would employ more rigorous wear testing would generate a larger number of samples for tests encompassing a broader range of motion path patterns. From such experiments, trends in the values of UHMWPE wear rates would be more reliably

generated and would be of a greater level of clinical significance. Additionally, a study of the morphology of wear particles generated from the various motion path patterns for both smooth and rough-counterface tests is also necessary (and forthcoming) to obtain a more accurate understanding of the wear mechanisms that are operative during the various wear paths. As mentioned previously, the presence of more sheet-like wear debris would indicate that significant reorientation occurs in the secondary direction of sliding. Therefore, a particle isolation study that aims to describe not only the morphology of debris particles but also quantifies the volume fractions of various particle morphologies would be valuable in elucidating the underlying mechanisms of wear in UHMWPE. In addition, the wear tests in this study employed a constant applied load of 192N and it is important for future studies to include wear test loading parameters which more closely model the variations in loading conditions found in knee and hip joints *in vivo*.

The relationship between wear path and wear rates established in this study applies only to uncrosslinked medical grade UHMWPE. Uncrosslinked UHMWPE was chosen specifically because volumetric wear rates and wear factors would be greater and trends in the effect of wear path geometry and counterface roughness would be more evident. Additionally, the process of crosslinking the UHMWPE prior to wear testing added an additional experimental variable and the goal of this study was to isolate the effects of cross-path motion and counterface roughness of wear behavior of UHMWPE. Because crosslinked UHMWPE is widely accepted in clinical use, further wear testing using the various forms of crosslinked UHMWPEs is required for such relationships to be established. This is particularly important as the process of crosslinking UHMWPE is known to affect the morphology of wear debris particles and the subsequent biologic

activity in response to wear debris [22]. This is an area of interest in the literature, and it has been shown that when using smooth femoral heads articulating against crosslinked UHMWPE, the wear rate was 30% lower than would be anticipated, but when the wear debris particles were isolated from serum and analyzed, it was found that there was a greater percentage volume of smaller, more biologically active particles [22]. Even though the volume of wear debris was substantially less than that found in tests that employed uncrosslinked UHMWPE, the larger percentage of small wear debris resulted in a similar index of biologic activity when compared with the non-crosslinked material [22]. In fact, direct cell culture studies of wear debris generated in wear simulators using multi-directional motion revealed a statistically significant increase in tumor necrosis factor-alpha levels and reactivity for GUR 1050 crosslinked polyethylene wear debris compared with an equivalent volume fraction of non-cross-linked GUR 1050 polyethylene [46].

Conclusions

Wear of UHMWPE, as it articulates against a metallic counterface in a particular wear path geometry and under conditions that mimic wear in a THR prosthesis, likely occurs via two discrete steps for rectangles with an aspect ratio greater than 2.3 (3mm×7mm rectangular path). For such rectangular wear paths, the wear tests of this study support the hypothesis that there is orientation or texturing of UHMWPE on parallel edges of the rectangle (principal sliding direction) followed by wear of the textured UHMWPE on the other two parallel edges (secondary direction of sliding). However, for rectangles in the aspect ratio range of 1.0–1.5 (5mm×5mm to 4mm×6mm

paths), the decline in wear rates for both smooth and rough-counterface experiments provide evidence that wear and orientation processes may not occur in discrete stages. In addition, the unified theory of wear model predicts zero wear for linear tracking, which is not the case, especially when more abrasive conditions of wear occur such as the case of a roughened-counterface. A more robust model is required to predict wear of UHMWPE during articulation against a metallic counterface along a rectangular path covering the entire range of aspect ratios of rectangles.

REFERENCES

[1] Charnley, J. 1963. *Tissue Reaction to the Polytetrafluoroethylene*. England: Lancet II. 1379 pp.

[2] Kurtz S., Mowat F., Ong K., Chan N., Lau E., *et al.* 2005. Prevalence of primary and revision total hip and knee arthroplasty in the United States from 1990 through 2002. *J. Bone Joint Surg. Am*. 87:1487–1497.

[3] Kurtz S., Stein H., Redeker G. 2005. Ultra-high-molecular-weight polyethylene has been the gold standard for 40 years. New technology and new materials can now offer even more options. Meeting the Joint Replacement Challenge with UHMWPE Material. *Medical Device & Diagn. Ind.* http://www.devicelink.com: March.

[4] Gomoll A., Wanich T., Bellare A. 2002. *J*-integral fracture toughness and tearing modulus measurement of radiation cross-linked UHMWPE, *J. Orthop. Res*. 20:1152-1156.

[5] Duus L., Walsh H., Gillis A., Noisiez E., Li S. 2000. The effect of resin grade, manufacturing method and cross linking on the fracture toughness of commercially available UHMWPE. *Trans. Orthop. Res. Soc.* 25:544. (Abstr.)

[6] Malchau H., Herberts P., Eisler T., Garellick G., Soderman P. 2002.The swedish total hip replacement register. *J. Bone Joint Surg.* 84A Suppl 2:2-20.

[7] Griffith M., Seidenstein M., Williams D., Charnley J. 1978. Socket wear in charnley low friction arthroplasty of the hip. *Clin. Orthop.* 137:37–47.

[8] Livermore J., Ilstrupand D., Morrey B. 1990. Effect of femoral head size on wear of the polyethylene acetabular component. *J. Bone Joint Surg.* 72A:518–528.

[9] Hall R., Unsworth A., Siney P., Wroblewski B. 1996. Wear in retrieved charnley acetabular sockets. *Proc. Inst. Mech. Eng. H: J. Eng. Med*. 210:197–207.

[10] Oonishi H., Tsuji E., Kim Y. 1998. Retrieved total hip prostheses. Part I. The effects of cup thickness, head size and fusion defects on wear. *J. Mater. Sci.: Mater. Med.* 9:394–401.

[11] Clarke I., Kabo J. 1991. *Wear in Total Hip Replacement, In: H.C. Amstutz (Ed.), Hip Arthroplasty*. New York: Churchill Livingstone.

[12] Lewis G. 1997. Polyethylene wear in total hip and knee arthroplasties. *J. Biomed. Mater. Res. (Appl. Biomater.)* 38:55–75.

[13] Amstutz H., Campbell P., Kossovsky N., Clarke I. 1992. Mechanisms and clinical significance of wear debris-induced osteolysis. *Clin. Orthop. Relat. Res.* 276:7–18.

[14] Harris W. 1995.The problem is osteolysis. *Clin. Orthop. Relat. Res.* 311:46–53.

[15] Schmalzried T., Kwong L., Jasty M., Sedlacek R., Haire T., *et al*. 1992. The mechanism of loosening of cemented acetabular components in total hip arthroplasty: analysis of specimens retrieved at autopsy. *Clin. Orthop. Relat. Res.* 274:60–78.

[16] Campbell P., Ma S., Yeom B., McKellop H., Schmalzried T., *et al*. 1995. Isolation of predominantly submicron-sized UHMWPE wear particles from periprosthetic tissues. *J. Biomed. Mater. Res.* 29:127–131.

[17] Shanbhag A., Jacobs J., Glant T., Gilbert J., Black J., *et al*. 1994. Composition and morphology of wear debris in failed uncemented total hip replacement. *J. Bone Joint Surg.* 76B:60–67.

[18] Savio J., Overcamp L., Black J. 1994. Size and shape of biomaterial wear debris. *Clin. Mater.* 15:101–119.

[19] Margevicius K., Bauer T., McMahon J., Brown S., Merritt K. 1994. Isolation and characterization of debris in membranes around total joint prostheses. *J. Bone Joint Surg.* 76A:1664–1676.

[20] Campbell P., Doorn P., Dorey F., Amstutz H. 1996. Wear and morphology of ultra-high molecular weight polyethylene wear particles from total hip replacements. *Proc. Inst. Mech. Eng. H: J. Eng. Med*. 210:167–175.

[21] Shanbhag A., Bailey H., Hwang D., Cha C., Eror N., *et al*. 2000. Quantitative analysis of ultrahigh molecular weight polyethylene (UHMWPE) wear debris associated with total knee replacements. *J. Biomed. Mater. Res*. 53:100–110.

[22] Endo M., Tipper J., Barton D., Stone M., Ingham E., *et al*. 2002. Comparison of wear, wear debris and functional biological activity of moderately crosslinked and non-crosslinked polyethylenes in hip prostheses. *Proc Inst Mech Eng [H]*. 216:111-22.

[23] Ramamurti B., Bragdon C., O'Connor D., Lowenstein J., Jasty M., *et al*. 1996. Loci of movement of selected points on the femoral head during normal gait. *J. Arthroplasty.* 11:852–855.

[24] Wang A., Sun D., Yau S., Edwards B., Sokol M., *et al*. 1997. Orientation softening in the deformation and wear of ultra-high polyethylene. *Wear*. 203–204:230–241.

[25] Saikko V., Ahlroos T. 1999. Type of motion and lubricant in wear simulation of polyethylene acetabular cup. *Proc. Inst. Mech. Eng. H: J. Eng. Med.* 213:301–310.

[26] Bragdon C., O'Connor D., Lowenstein J, Jasty M., Syniuta W. 1996. The importance of multidirectional motion on the wear of polyethylene. *Proc. Inst. Mech. Eng. H: J. Eng. Med.* 210:157–166.

[27] Wang A., Stark C., Dumbleton J. 1996. Mechanistic and morphological origins of ultra-high molecular weight polyethylene wear debris in total joint replacement prostheses. *Proc. Inst. Mech. Eng. H: J. Eng. Med.* 210:141–155.

[28] Wang A., Polineni V., Essner A., Sokol M., Sun D., *et al*. 1997. The significance of non-linear motion in the wear screening of orthopaedic implant materials. *Test. Eval.* 25:239–245.

[29] Wang A., Essner A., Polineni V., Stark C., Dumbleton J. 1998. Lubrication and wear of ultra-high molecular weight polyethylene in total joint replacements. *Tribol. Int.* 31:17–33.

[30] Caravia L., Dowson D., Fisher J., Jobbins B. 1990. The influence of bone and bone cement debris on counterface roughness in sliding wear tests of ultra-high molecular weight polyethylene on stainless steel. *Proc. Inst. Mech. Eng. H: J. Eng. Med.* 204:65–70.

[31] Brown T., Stewart K., Nieman J., Pedersen D., Callaghan J. 2002. Local head roughening as a factor contributing to variability of total hip wear: a finite element analysis. *J. Biomech. Eng.*124:691–698.

[32] Bennett D., Orr J., Baker R. 2000.Movement loci of selected points on the femoral head for individual total hip arthroplasty patients using three-dimensional computer simulation. *J. Arthroplasty.* 15:909–915.

[33] Wang A. 2001. A unified theory of wear for ultra-high molecular weight polyethylene in multidirectional sliding. *Wear.* 248:38–47.

[34] Turell M., Wang A., Bellare A. 2003. Quantification of the effect of cross-path motion on the wear rate of ultra-high molecular weight polyethylene. *Wear.* 255:1034–1039.

[35] Marti A., Schmid A., Bigolin G., Schmid H. 2002. Evaluation and assembly of a test set-up for tribological investigations. *RMS-Report*. p.15.

[36] Rezaei M., Shirzad A., Ebrahimi N., Kontopoulou M. 2005. Surface modification of ultra-high-molecular-weight polyethylene. II. Effect on the physiomechanical and tribological properties of ultra-high-molecular-weight polyethylene/poly(ethylene terephthalate) composites. *J. Appl. Polym. Sci.* 99:2352–2358.

[37] Mazzucco D., Spector M. 2006. Contact area as a critical determinant in the tribology of metal-on-polyethylene total joint arthroplasty. *J. Tribol*. 128:113-121

[38] Brand R., Iglič A., Kralj-Iglič V. 2001. Contact stresses in the human hip: Implications for disease and treatment. *Hip Internl*. 11:117-126

[39] Brand R. 2005. Joint contact stress: a reasonable surrogate for biological processes. *Iowa Orthop. J.*. 25:82-94

[40] Polineni V., Wang A., Essner A., Stark C., Dumbleton J. 1997. Effect of lubricant protein concentration on the wear of UHMWPE acetabular cups against cobalt-chrome and alumina femoral heads. *Trans 23rd Annual Meeting of the Society for Biomaterials*. 23:154 (Abstr.)

[41] Wang A., Polineni V., Essner A., Stark C., Dumbleton J. 1999. The impact of lubricant protein concentration on the outcome of hip joint simulator testing. *48th Annual Meeting of the Orthopedic Research Society*. 48:52 (Abstr.)

[42] Wang A., Polineni V., Essner A., Stark C., Dumbleton J. 1998. Role of proteins and hyaluronic acid in the lubrication and wear of UHMWPE acetabular cups. *Trans 24th Annual Meeting Society for Biomaterials*. 24:218 (Abstr.)

[43] Wang A. , Essner A., Schmidig G. 2004. The effects of lubricant composition on *in vitro* wear testing of polymeric acetabular components. *J. Biomed. Mater. Res. Part B: Appl. Biom*. 68B:45-52

[44] Wang A., Polineni V., Stark C., Dumbleton J. 1998. Effect of femoral head surface roughness on the wear of ultrahigh molecular weight polyethylene acetabular cups. *J. Arthroplasty*. 6:615–620

[45] Nusbaum H., Rose R. 2004. The effects of radiation sterilization on the properties of ultrahigh molecular weight polyethylene. *J. Biomed. Mater. Res*. 13:557-576

[46] Fisher J., McEwen H., Tipper J., Galvin A., Ingram J., *et al*. 2004. Wear, debris, and biologic activity of cross-linked polyethylene in the knee: benefits and potential concerns. *Clin. Orthop. Relat. Res.* 428:114-119